*Transactions of the Materials Research Society of Japan* 29[4] 1135-1138 (2004)

# 500MHz-18GHz Microwave Absorber Using Magnetic-Dielectric Composite Material

Takashi Miura, Hirotake Okino and Takashi Yamamoto
Department of Communications Engineering, National Defense Academy
1-10-20 Hashirimizu, Yokosuka, Kanagawa 239-8686 Japan
Fax: +81-46-844-5911, e-mail: g41012@nda.ac.jp

Microwave absorber is a necessary device for the application of high frequency (MHz-GHz) for eliminating a miss-operation of precise electronic equipment and outflow of secret information occurred by a leakage of electromagnetic wave. We present the accurate measurement method of complex permeability and permittivity in 500MHz-18GHz. Design of the microwave absorber using complex permeability and permittivity is demonstrated using the magnetic (Carbonyl iron, $Fe(CO)_5$, called "Fe" for short) and dielectric (Titanium oxide, $TiO_2$, called "Ti" for short) composite material. By changing the composition ratio of magnetic/dielectric in the composite and the sample thickness, the 99.9% of electromagnetic wave could be eliminated in the frequency range from 5.7GHz to 13.9GHz, where this frequency range is depended on material composition, that is, the frequency dependence of permeability and permittivity of this material. Additionally, we represent the TE-TM polarized wave characteristics of the magnetic-dielectric composite microwave absorber. The comparison for experimental results and theory are presented and discussed for the microwave absorber for ETC (Electronic Toll Collection) system.

Key words: Microwave Absorber, Complex Permeability and Permittivity, TE-TM Polarized Wave

## 1. INTRODUCTION

Recently, we begin to use the high frequency for ETC (5.8GHz in Japan), Wireless LAN (2GHz~60GHz), and ITS (~70GHz), personal digital assistant (800MHz~2GHz) and Bluetooth (2.4GHz). The used frequency is expanded from MHz to GHz. Many problems have been occurred along with it. Therefore, the improvement of the electromagnetic radiation environment at each frequency is requested and the microwave absorber is needed. Microwave absorber using a ferrite showed excellent microwave absorbing characteristics in the MHz band.[1] However, ferrite has not given a sufficient absorption in the high frequency GHz band because of Sneok's low.[2] Therefore we designed a microwave absorber using the magnetic-dielectric composite material and evaluated its characteristics.

## 2. THEORY

### 2.1 Through Method using Coaxial Line [3]

When a transverse electromagnetic wave (TEM wave) is at vertical incidence to a microwave absorber as shown in Fig.1 (a), it is possible to treat it as an equivalent distributed constant circuit shown in Fig.1 (b). In this way, $Z_C$ is the characteristic impedance, $\gamma$ the propagation constant, and d the thickness of the microwave absorber. When the reflection coefficient and transmission coefficient, which the measurement reference planes are settled at a position on reference planes 1 and 2 in Fig.1 (b), is assumed to be $S'_{11}$ and $S'_{21}$, the reflection coefficient $S_{11}$ and transmission coefficient $S_{21}$ with the sample is given by equations (1) and (2). Measured $S_{11}$ and $S_{21}$ are given by equations (3) and (4) by using the characteristic impedance $Z_C$ and the propagation constant $\gamma$ of the sample from the transmission theory. Therefore, $Z_C$ and $\gamma$ are calculated from equations (5) and (6) by using measured $S_{11}$ and $S_{21}$.

$$S_{11}=S'_{11}e^{-2j\varphi_1} \tag{1}$$

$$S_{21}=S'_{21}e^{j(\varphi_1+\varphi_2)} \tag{2}$$

$$S_{11}=\frac{(1-Z_C^2)(1-\exp(-2\gamma d))}{(1+Z_C)^2-(1-Z_C)^2\exp(-2\gamma d)} \tag{3}$$

$$S_{21}=\frac{4Z_C\exp(-2\gamma d)}{(1+Z_C)^2-(1-Z_C)^2\exp(-2\gamma d)} \tag{4}$$

$$Z_C=\pm\frac{\sqrt{(1-S_{11}^2+S_{21}^2)^2-4S_{21}^2}}{(1-S_{11})^2-S_{21}^2} \tag{5}$$

$$\gamma=-\frac{1}{d}\left(\log\frac{1-S_{11}^2+S_{21}^2-\left\{(1-S_{11})^2-S_{21}^2\right\}Z_C}{2S_{21}}+2n\pi\right) \tag{6}$$

$$\mu_r^*=\mu'-j\mu''=-j\frac{\lambda_0}{2\pi}Z_C\gamma \tag{7}$$

$$\varepsilon_r^*=\varepsilon'-j\varepsilon''=-j\frac{\lambda_0}{2\pi}\frac{\gamma}{Z_C} \tag{8}$$

where, n is the integer. Therefore, complex permeability $\mu^*_r$ and permittivity $\varepsilon^*_r$ are calculated by using equations (7) and (8).

2.2 Calibration

The calibration in the experiment used the OSL (Open-Short-Load) method in 1GHz-18GHz and the TRL (Thru-Reflect-Line) method in 1GHz or less. To calibrate two ports, the OSL method corrects the error of full 12-terms by using the precision standard Open, Short, and Load (Termination) and the TRL method uses two lines and a reflection. The OSL and TRL method can remove the error of the system including the measurement device by measuring these.

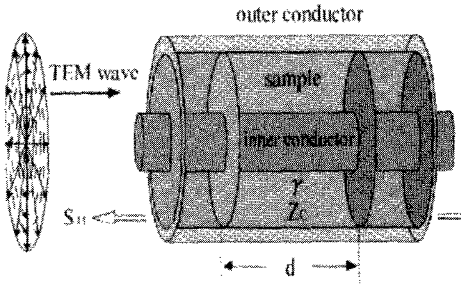

Fig.1 (a) through method

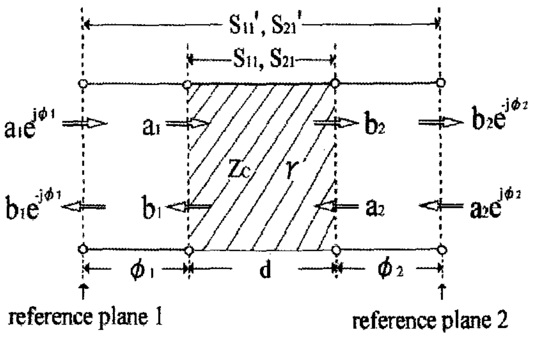

Fig.1 (b) equivalent circuit

3. SAMPLE

Carbonyl iron ($Fe(CO)_5$) powder was used as the magnetic material, and titanium oxide ($TiO_2$) powder as the dielectric material. The mean particle diameter of both was about 3.6$\mu$m. They were mixed with hyparon in various mixing ratio, and molded in a toroidal shape, which could be inserted in 7D and 20D coaxial wave-guide.

Table.I: Fe/Ti weight-mixing ratios for the magnetic and dielectric composite samples

| Fe/Ti ratio (wt%) | Fe | Ti | hyparon | Packing factor | characteristics |
|---|---|---|---|---|---|
| 100/0 | 500g | - | 100g | 83.3% | magnetic |
| 90/10 | 450g | 50g | 100g | 83.3% | magnetic>dielectric |
| 80/20 | 400g | 100g | 100g | 83.3% | magnetic>dielectric |
| 70/30 | 350g | 150g | 100g | 83.3% | magnetic≒dielectric |
| 60/40 | 300g | 200g | 100g | 83.3% | magnetic≒dielectric |
| 50/50 | 250g | 250g | 100g | 83.3% | magnetic=dielectric |

The properties were changed from magnetic to dielectric by changing the weigh-mixing ratio (composition ratio) from Fe/Ti=100/0 to Fe/Ti=50/50. The entire filling fraction is 83.3%, and the remainder of 16.7% is the hyparon. Table.I shows the Fe/Ti weight-mixing ratios in the composite materials.

4. RESULTS AND DISCUSSION

4.1 Measurement of Complex Permeability ($\mu^*_r=\mu'-j\mu''$) and Permittivity ($\varepsilon^*_r=\varepsilon'-j\varepsilon''$)

Figure 2 (a) and (b) show the frequency dependence of complex permeability ($\mu^*_r=\mu'-j\mu''$) and permittivity ($\varepsilon^*_r=\varepsilon'-j\varepsilon''$) for Fe/Ti=60/40 in 500MHz to 1GHz. Figure 3 (a) and (b) show the frequency dependence of complex permeability ($\mu^*_r=\mu'-j\mu''$) and permittivity ($\varepsilon^*_r=\varepsilon'-j\varepsilon''$) for Fe/Ti=60/40 in 1GHz to 18GHz. In 500MHz to 1GHz, the $\mu'$ gradually decreases and inversely the $\mu''$ gradually increases. The $\varepsilon'$ is almost constant, however the $\varepsilon''$ gradually decreases. In 1GHz to 18GHz, the $\mu'$ gradually decreases on high frequency range, though the $\mu''$ is almost constant. On the other hand, the $\varepsilon'$ is almost constant and the $\varepsilon''$ increases on high frequency range.

Table.II shows the $\mu'$, $\mu''$, $\varepsilon'$, and $\varepsilon''$ at 5.8GHz. As the content of dielectric material in this composite decrease, the $\mu'$ and $\mu''$ increase, the $\varepsilon'$ and $\varepsilon''$ decrease.

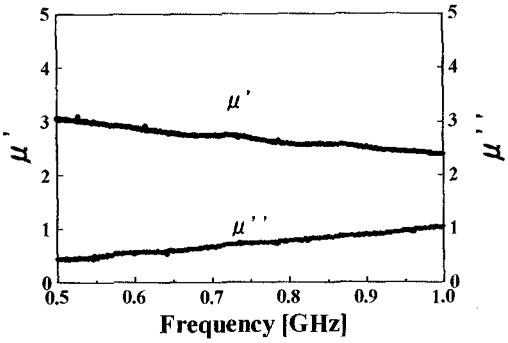

Fig.2 (a) complex permeability ($\mu^*_r=\mu'-j\mu''$) in 500MHz-1GHz

(Fe/Ti=60/40, thickness=2.4mm, 20D coaxial)

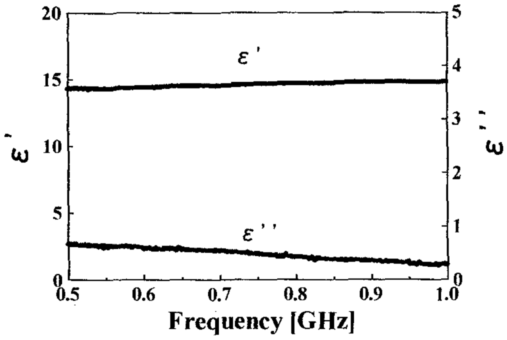

Fig.2 (b) complex permittivity ($\varepsilon^*_r=\varepsilon'-j\varepsilon''$) in 500MHz-1GHz

(Fe/Ti=60/40, thickness=2.4mm, 20D coaxial)

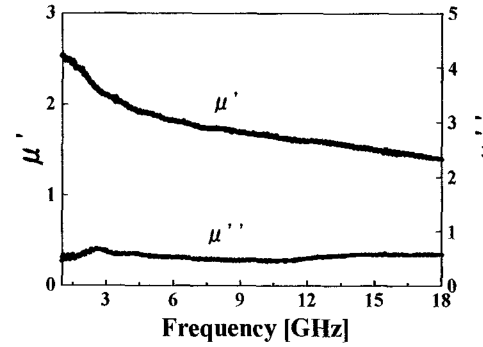

Fig.3 (a) complex permeability ($\mu^*_r=\mu'-j\mu''$) in 1GHz-18GHz

(Fe/Ti=60/40, thickness=2.4mm, 7D coaxial)

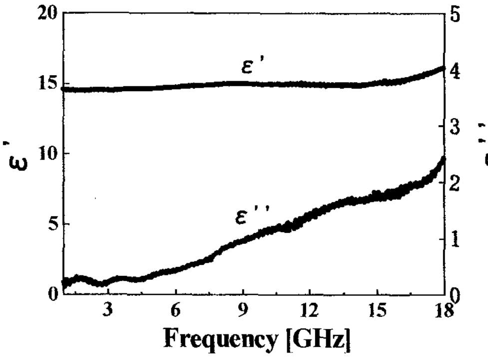

Fig.3 (b) complex permittivity ($\varepsilon^*_r=\varepsilon'-j\varepsilon''$) in 1GHz-18GHz

(Fe/Ti=60/40, thickness=2.4mm, 7D coaxial)

Table.II: complex permeability ($\mu^*_r=\mu'-j\mu''$) and permittivity ($\varepsilon^*_r=\varepsilon'-j\varepsilon''$) at 5.8GHz changed Fe/Ti weight-mixing ratio from 100/0 to 50/50

| Fe/Ti ratio (wt%) | $\mu'$ | $\mu''$ | $\varepsilon'$ | $\varepsilon''$ |
|---|---|---|---|---|
| 100/0 | 2.55 | 2.07 | 16.11 | 0.29 |
| 90/10 | 2.36 | 1.32 | 14.84 | 0.29 |
| 80/20 | 2.12 | 1.01 | 14.57 | 0.24 |
| 70/30 | 1.93 | 0.78 | 15.77 | 0.21 |
| 60/40 | 1.82 | 0.53 | 14.71 | 0.41 |
| 50/50 | 1.62 | 0.37 | 14.12 | 0.32 |

### 4.2 Reflection Loss at the Matching Frequency

The frequency dependence of the reflection loss of the single-layer microwave absorber is calculated by using measured $\mu^*_r$ and $\varepsilon^*_r$. The characteristic impedance $Z_C$ is given by equation (9), and the propagation constant $\gamma$ is given by equation (10). Though the normalized impedance $Z_{in}$ of the sample is given by equation (11), when the terminal is a short, equation (11) becomes equation (12) because $Z_L$ is ideally 0. Because the reflection coefficient $S_{11}$ is given by equation (13), the reflection loss $\Gamma_{11}$ is given by equation (14). When the electric field is at vertical incidence to the sample, the characteristic impedance $Z_C$ of TE wave is given by equation (15). Similarly, when the magnetic field is at vertical incidence to the sample, the characteristic impedance $Z_C$ of TM wave is given by equation (16). Therefore, the propagation constant $\gamma$ is given by equation (17) and the reflection loss $\Gamma_{11}$ of TE wave and TM wave are given by equations (18) and (19).

$$Zc=\sqrt{\frac{\mu_r^*}{\varepsilon_r^*}} \qquad (9)$$

$$\gamma=j\frac{2\pi}{\lambda_0}\sqrt{\mu_r^*\varepsilon_r^*} \qquad (10)$$

$$Z_{in}=Zc\frac{Z_L+Zc\tanh\gamma d}{Zc+Z_L\tanh\gamma d} \qquad (11)$$

$$Z_{in}=Zc\tanh\gamma d \qquad (12)$$

$$S_{11}=\frac{Z_{in}-1}{Z_{in}+1} \qquad (13)$$

$$\Gamma_{11}=20\log S_{11} \qquad (14)$$

$$Zc=\frac{\mu r^*}{\sqrt{\mu r^*\varepsilon r^*-\sin^2\theta}} \quad \text{(TE theory)} \qquad (15)$$

$$Zc=\frac{\sqrt{\mu r^*\varepsilon r^*-\sin^2\theta}}{\varepsilon r^*} \quad \text{(TM theory)} \qquad (16)$$

$$\gamma=j\frac{2\pi}{\lambda_o}\sqrt{\mu r^*\varepsilon r^*-\sin^2\theta} \qquad (17)$$

$$\Gamma_{11}=20\log\left|\frac{Zin-1/\cos\theta}{Zin+1/\cos\theta}\right| \quad \text{(TE theory)} \qquad (18)$$

$$\Gamma_{11}=20\log\left|\frac{Zin-\cos\theta}{Zin+\cos\theta}\right| \quad \text{(TM theory)} \qquad (19)$$

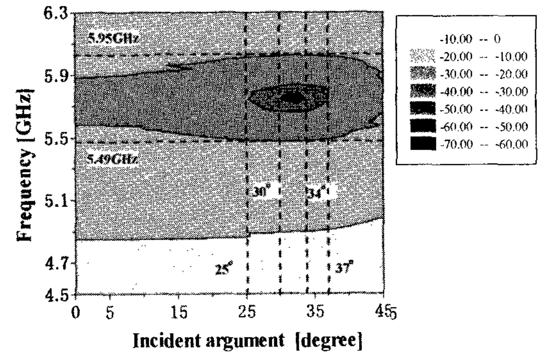

Fig.4 (a) Oblique projection dependence of the single-layer microwave absorber (TE wave)

(Fe/Ti=60/40, thickness=2.35mm)

Figure 4 (a) shows the matching frequency and the reflection loss at the matching frequency calculated by using equations (15), (17) and (18) from $\mu^*_r$ and $\varepsilon^*_r$ in TE wave of Fe/Ti=60/40 with a sample thickness of 2.35mm. When the matching frequency is 5.62GHz and the incident angle is $\theta$i=0° to 45°, the reflection loss is -20dB or more. Figure 4 (b) shows the matching frequency and the reflection loss at the matching frequency calculated by using equations (16), (17) and (19) from $\mu^*_r$ and $\varepsilon^*_r$ in TM wave of Fe/Ti=60/40 with a sample thickness of 2.35mm. When the matching frequency is 5.8GHz and the incident angle is θi=0° to 14°, the reflection loss is -20dB or more.

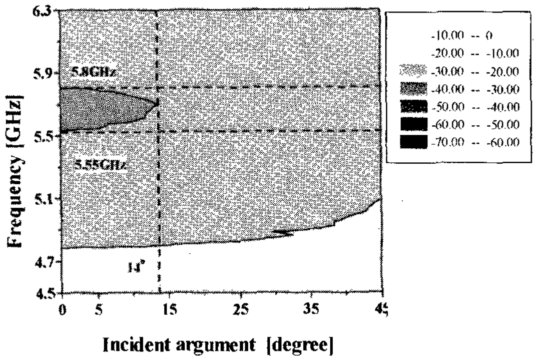

Fig.4 (b) Oblique projection dependence of the single-layer microwave absorber (TM wave)
(Fe/Ti=60/40, thickness=2.35mm)

### 4.3 Reflection Loss at the Matching Frequency in the Free Space

Reflection loss at the matching frequency in the free space is measured by using the measurement system as shown in Fig.5. The measurement is used in the anechoic chamber to reduce the influence of the reflection electromagnetic radiation from a surrounding reflection body and the time domain to remove unnecessary scattered wave. The TE wave and TM wave characteristic of the sample were measured by attaching the transmission and the receive antenna in a wooden arch. Reflection loss is measured by the difference between the reflection loss of a metallic board of the same size as the sample and the sample to put the metallic board on the back.

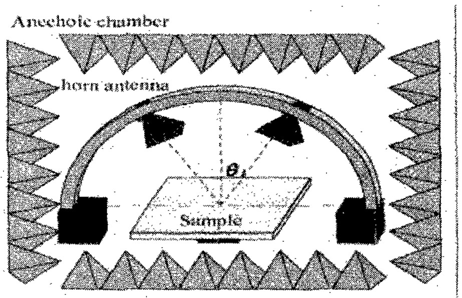

Fig.5 measurement in the free space

Figure 6 (a) and (b) show the frequency dependence of the reflection loss in 4GHz-6GHz of Fe/Ti=60/40 with a sample thickness of 2.35mm for TE wave and TM wave at the incident angle of 30° . In the calculated value of Fig.6 (a), the matching frequency is 5.6GHz, and the reflection loss is –36dB. On the other hand, the matching frequency is 5.6GHz, and the reflection loss is –32dB in the experimental value of Fig.6 (a). In the calculated value of Figure 6 (b), the matching frequency is 5.7GHz, and the reflection loss is –16.4dB. On the other hand, the matching frequency is 5.7GHz, and the reflection loss is –15.7dB in the experimental value of Fig.6 (b). The calculated value and the experimental value showed a good agreement. Therefore, the matching frequency and the reflection loss can be forecast by obtaining complex permeability $\mu^*_r$ ($\mu'$, $\mu''$) and permittivity $\varepsilon^*_r$ ($\varepsilon'$, $\varepsilon''$), and the microwave absorber can be designed.

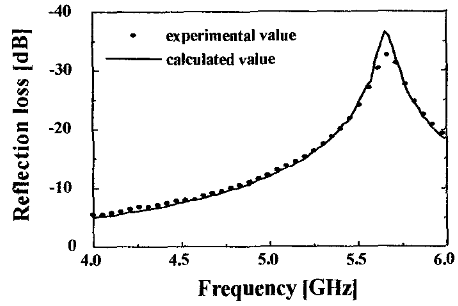

Fig.6 (a) comparison with calculated and experimental data of the reflection loss
(TE wave, incident angle=30° )
(Fe/Ti=60/40, thickness=2.35mm)

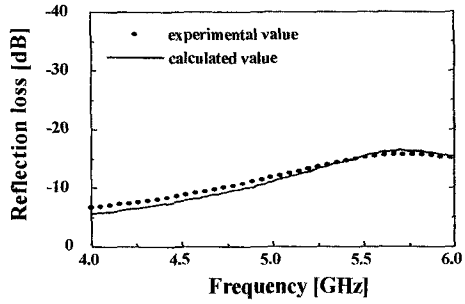

Fig.6 (b) comparison with calculated and experimental data of the reflection loss
(TM wave, incident angle=30° )
(Fe/Ti=60/40, thickness=2.35mm)

## 5. CONCLUSION

(1) Frequency dependence of complex permeability $\mu^*_r$ ($\mu'$, $\mu''$) and permittivity $\varepsilon^*_r$ ($\varepsilon'$, $\varepsilon''$) of the magnetic-dielectric composite material in 500MHz-18GHz were obtained by the through method in the coaxial wave-guide with a network analyzer.

(2) It has given the good agreement between experimental and calculated matching frequency and reflection loss.

## 6. REFERENCES

[1] Y.Naito "Wave absorber" Ohm Co., pp-55, (1998) in Japanese

[2] M.Saito, T.Yamamoto, T.Sakamoto, H.Niori, M.Chino and M.Kobayashi, "Electromagnetic wave absorber using dielectric-magnetic composite material for GHz frequency band (I)" Proc. of IEEE, ISAF, (2000)

[3] A.M.Nicolson, et. al, "Measurement of the Intrinsic Properties of Materials by Time-Domain Techniques" IEEE Trans Inst and Measurement. Vol.IM-19, No.4, pp377-382

(Received October 11, 2003; Accepted March 10, 2004)